Optical-televiewer-based logging of the uppermost 630 m of the NEEM deep ice borehole, Greenland

Bryn HUBBARD, Terry MALONE

Centre for Glaciology, Institute of Geography and Earth Sciences, Aberystwyth University, Aberystwyth, UK
E-mail: byh@aber.ac.uk

ABSTRACT. We report on the application of optical televiewing (OPTV) to the uppermost 630 m of the North Greenland Eemian Ice Drilling (NEEM) deep ice borehole, Greenland. The resulting log reveals numerous natural and drilling-related properties, including the integrity of the borehole casing and its joints, the presence of drill-tooth scoring on the ice wall of the borehole and the presence of regularly repeated layering, interpreted to be annual, to a depth approaching 200 m. A second OPTV log was acquired from a nearby shallow borehole. With the exception of the uppermost ~10 m, this log shows a gradual decrease in luminosity with depth, interpreted as a decrease in light scattering with firnification. This shallow log also clearly images annual layers, allowing the construction of an age–depth scale. Comparing this with an independent core-based scale reveals that the OPTV record yields an age of 1724 at the deepest common point of both scales (80 m), 13 years older than the core-based record at 1737. However, all of this deviation accrues in the uppermost ~30 m of the OPTV record where highly reflective snow saturates the luminosity of the borehole image, an artefact that can be reduced by further adaptation of the OPTV system.

1. INTRODUCTION

Digital optical televiewing (OPTV) has been developed over the past decade primarily for borehole inspection and analysis associated with mineral exploration (e.g. Siddans, 2002). However, the technique also shows great promise in imaging the snow, firn and ice layers intersected by boreholes drilled through ice masses (e.g. Hubbard and others, 2008, 2012; Roberson and Hubbard, 2010; Obbard and others, 2011). OPTV differs from traditional directional borehole video in that it records, at millimetric resolution, a 360° annular image of the complete borehole circumference. These annuli are then stacked – guided by precise depth control – to produce an orientated, geometrically accurate image of a complete borehole wall. The benefits of OPTV relate both to this complete coverage and to its ability to recreate the geometrical properties of any visibly identifiable object or layer that intersects a logged borehole. Planes intersecting logged boreholes appear as sinusoids on the raw OPTV images, and the dip and dip direction of each such plane can be calculated from the amplitude and phase, respectively, of its associated sinusoid. This geometrical accuracy also allows raw OPTV images to be rolled and inverted to produce virtual core images, even from boreholes from which no actual core was retrieved. Finally, OPTV views radially outwards into the ice surrounding a borehole. It thereby provides a deep-field image with the capacity to reveal properties that may not be intersected by, or easily identifiable from, analysis of a core that is typically 8–10 cm in diameter. Below the uppermost few metres this recorded light is composed exclusively of that reflected back from the borehole walls to the OPTV sensor. Since borehole illumination is constant, the brightness of the signal recorded by the OPTV camera varies with the reflectivity of the material forming the borehole wall.

Given these characteristics it is evident that OPTV can potentially contribute to deep ice-drilling programmes both as an inspection tool, imaging drilling-related artefacts, and as an investigative tool, imaging natural material properties. The aim of this paper is to evaluate these contributions by reference to two OPTV logs, one from the uppermost 630 m of the North Greenland Eemian Ice Drilling (NEEM) deep ice borehole, Greenland, and the other from a nearby 87 m long shallow borehole.

2. FIELD SITE AND METHODS

The NEEM site is located at ~2485 m a.s.l. on an elongated surface crest between the North Greenland Icecore Project (NorthGRIP) and Camp Century in the northwestern sector of the Greenland ice sheet (77.45° N, 51.06° W) (http://neem.dk/). Net mass accumulation in the area is ~0.2 m w.e. a^{-1} (Kuramoto and others, 2011; Steen-Larsen and others, 2011). The deep borehole was cored through the summers of 2009 and 2010 using a Hans-Tausen-type electromechanical corer, retrieving 98 mm diameter core from a borehole with a diameter of between 126 (dry) and 130 mm (wet) (Johnsen and others, 2007). The uppermost section of borehole was cased to prevent the possible loss of drilling fluid (an Estisol–Coasol mix) into the ice sheet's permeable firn layer. The ice-sheet base was reached at a depth of ~2537 m below the surface on 27 July 2010, revealing the presence of ~1 m of debris-rich basal ice located immediately above the ice–bed interface.

OPTV logging was carried out at the NEEM site during July and August 2010 using an adapted probe and micrologger system manufactured by Robertson Geologging Ltd, as described by Hubbard and others (2008) (Fig. 1). The system comprises three units: the ~2.0 m long probe, a surface laptop and micrologger, and a winch spooled with 650 m of 3/16 inch (1 inch = 2.54 cm) four-core cable, weighing ~225 kg in total. In order to ensure radial symmetry the 58 mm diameter probe was centralized in the ~130 mm diameter hole using two four-arm centralizers (Fig. 1). Two OPTV logs were recovered: the first of the uppermost 630 m

https://doi.org/10.3189/2013AoG64A201 Published online by Cambridge University Press

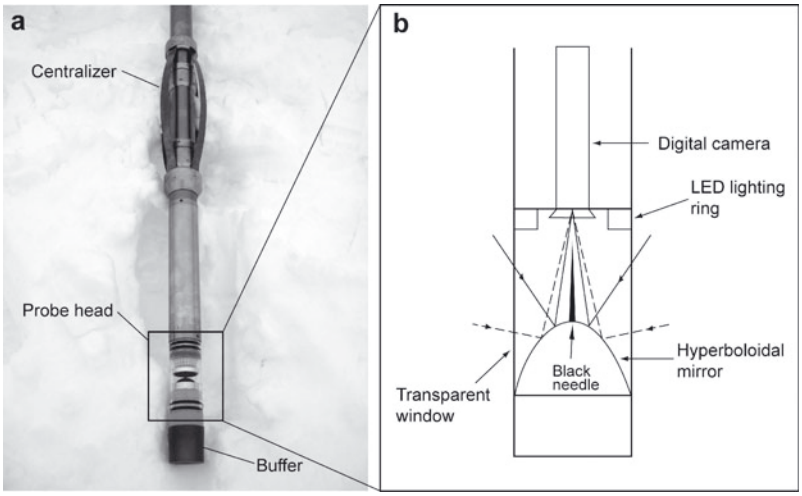

Fig. 1. The optical televiewer used in this study represented as (a) a photographic image and (b) a sketch expansion of the probe's key components.

of the principal deep borehole and the second to 87 m depth in a nearby shallow borehole. The former log was restricted to a length of ~630 m by available hardware and signal-processing capability, both of which have now been overcome allowing future logs to be recovered from up to 3 km depth. The shallow log provided a near-surface OPTV record that was unobtainable from the deep borehole due to it being cased over this depth range. Both logs were recovered at a logging speed of ~1 m min^{-1}, yielding an along-borehole resolution of 1.0 mm per pixel and an around-borehole resolution of 720 pixels per row (i.e. ~0.6 mm per pixel).

Once logged, OPTV images were collated, analysed and prepared for presentation (including rolling to create virtual core images) using WellCad software. This analysis included calculating the luminosity (expressed in non-dimensioned units of RGB pixel brightness) of each depth step, represented by the mean value of each ring of 720 pixels.

3. RESULTS

3.1. NEEM deep borehole

The OPTV log of the uppermost 630 m of the deep borehole (Figs 2 and 3) reveals several noteworthy properties, both natural and drilling-related. Beginning at a log depth of 10 m the casing is clearly imaged through the air-filled upper borehole (Fig 3a), showing vertical stripes where the drill centralizers have scored the casing material. Joints between individual casing sections are also clearly visible, mostly as horizontal planes (indicating a similar geometry in reality). However, the join located at a log depth of ~79 m appears as a sinusoid on the raw OPTV log (Fig 3a). Analysis of the dip and dip direction of this sinusoid indicates that this particular casing joint dips by ~17° in the direction ~205°. In contrast, the upper surface of the borehole fluid, imaged at a log depth of ~91.8 m, forms a horizontal plane (Fig 3b). Although expected, this record of the fluid surface being perfectly planar and horizontal verifies the calibration of the OPTV instrument. Immediately below the fluid level, Figure 3b reveals that the image is obscured, with light reflection from the borehole wall being severely disrupted locally. This effect appears to be caused by the presence of an amorphous mass of reflective material within the borehole fluid, almost certainly buoyant ice chips that have escaped from the borehole baler and aggregated at the surface of the fluid column.

Within the fluid-filled borehole, the OPTV image appears dark and homogeneous relative to shallower borehole records of snow and firn (below) and those recovered from more compositionally varied settings such as valley glaciers (Hubbard and others, 2008; Roberson and Hubbard, 2010) and ice-shelf rifts (Hubbard and others, 2012). Despite this compositional homogeneity within the ice in the uppermost few hundred metres of the NEEM borehole, layers are occasionally visible in the OPTV record. For example, at ~165 m depth (Fig. 3c), several horizontal layers can be seen over some decimetres. These light and dark layers repeat regularly through this zone, with the lighter layers being thicker than the darker layers and the two showing a typical spacing of ~0.05 m. The regularity and spacing of these layers strongly suggest that they are annual (cf. analysis of shallow borehole OPTV log in Section 3.2).

As well as regular layering, the deep borehole OPTV log also reveals the presence of regular patterning on the borehole wall over several decimetre- to metre-long sections between 170 and 190 m (e.g. Fig 3d). These do not form sinusoids, but straight, consistently dipping planes that cut across each other, forming what appears to be a sawtooth pattern. The straightness of these planes indicates that they form a helical pattern along the curved borehole wall, consistent with scores formed by the cutting teeth of the ice corer. This interpretation accords with NEEM drill records reporting that the cutters were changed at this depth.

3.2. NEEM shallow borehole

OPTV was also used to log the uppermost 87 m of the ice sheet via a shallow borehole drilled within a few kilometres of the principal deep borehole. This presented the opportunity to complement the deep-hole OPTV log with coverage of the snow–firn–ice transition otherwise obscured by casing in the deep hole. The resulting OPTV log (Fig. 4) is brighter and shows far more internal structure than that of the deep borehole (Fig. 2).

Perhaps the most apparent aspect of the shallow borehole log is its general decrease in brightness with depth, from typical luminosity values of ~250 near the surface to <150 at its base. Similar decreases in luminosity have been

https://doi.org/10.3189/2013AoG64A201 Published online by Cambridge University Press

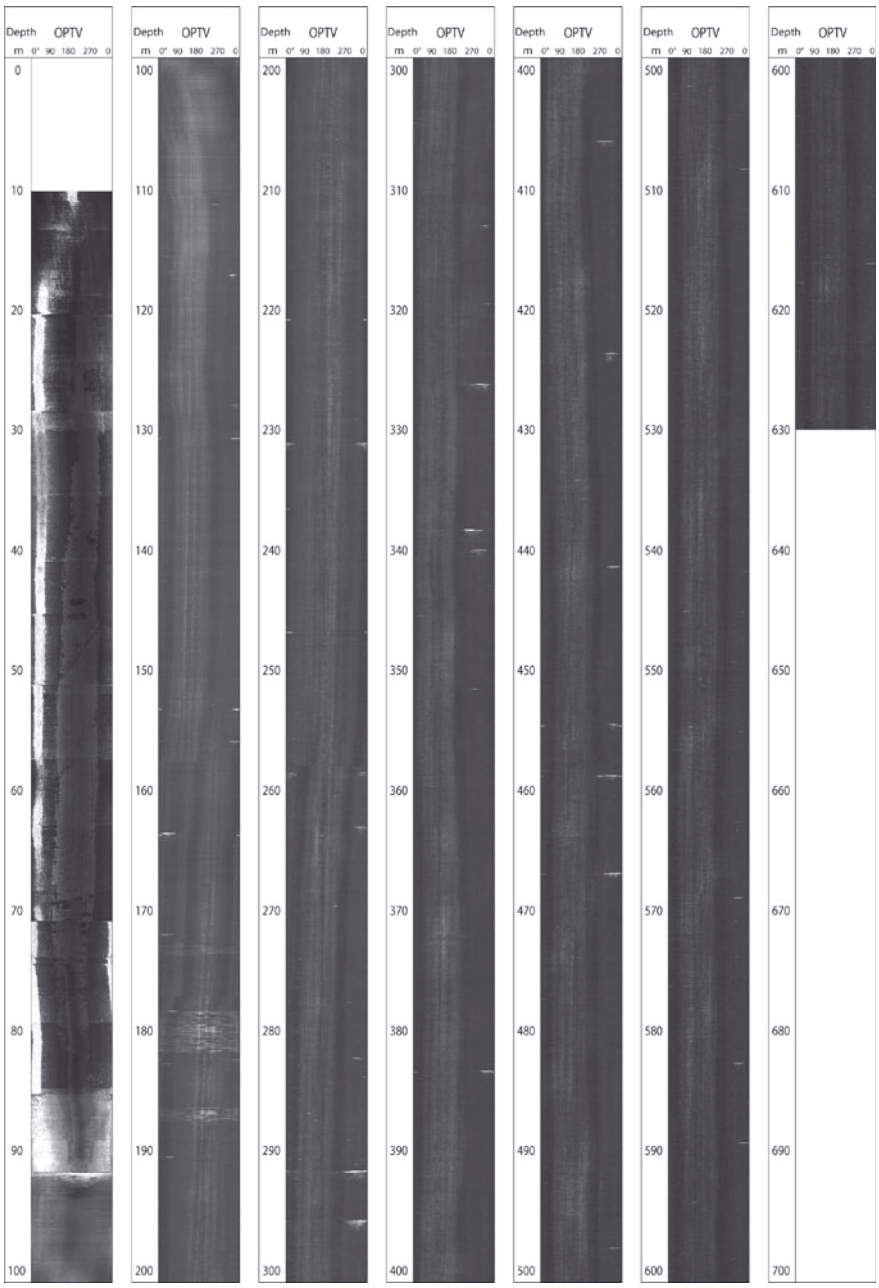

Fig. 2. Complete raw OPTV log of the uppermost 630 m of the NEEM deep ice borehole. Note that the quasi-vertical stripes on the record are scores caused by the drill centralizers as it was raised and lowered along the borehole.

reported elsewhere, including in the optical analysis of a firn core (e.g. Kinnard and others, 2008), in the video analysis of boreholes drilled in firn (e.g. Hawley and Morris, 2006) and, recently, in OPTV logs of an Antarctic ice shelf (Hubbard and others, 2012). In each case, this general decrease in light reflectance (or increase in transmission) over the visible spectrum is attributed to the gradual nucleation and eventual exclusion of air bubbles during firnification. In generating such luminosity profiles, OPTV logging thereby provides a potential means of approximating snow and firn density. One interesting aspect of the general luminosity trace illustrated in Figure 4 is that the trend towards decreasing luminosity with depth is reversed in the uppermost ~10 m (i.e. luminosity increases with depth through the top 10 m). This effect has also been reported by others, for example in a video-based analysis of a shallow borehole drilled at Summit, Greenland, by Hawley and Morris (2006). Those authors followed Bohren and Barkstrom (1974) in interpreting this inversion in terms of densification by grain-boundary sliding in this near-surface low-density zone (shallower than ~15 m in the Summit data). This process generates a net increase in total scattering area with density, and hence depth, up to the point at which further densification by pressure sintering dominates (>~0.5 g cm^{-3}). Thereafter, a negative relationship between scattering and density is expected (Bohren and Barkstrom, 1974). This interpretation is consistent with the general luminosity characteristics of the shallow borehole log reported herein and illustrated in Figure 4. Precise comparison of OPTV luminosity and snow/firn density is not possible for the NEEM shallow hole because density data are not available for this core at a sufficiently high resolution for detailed comparison. However, this potential is being investigated in detail as part of ongoing studies based on

https://doi.org/10.3189/2013AoG64A201 Published online by Cambridge University Press

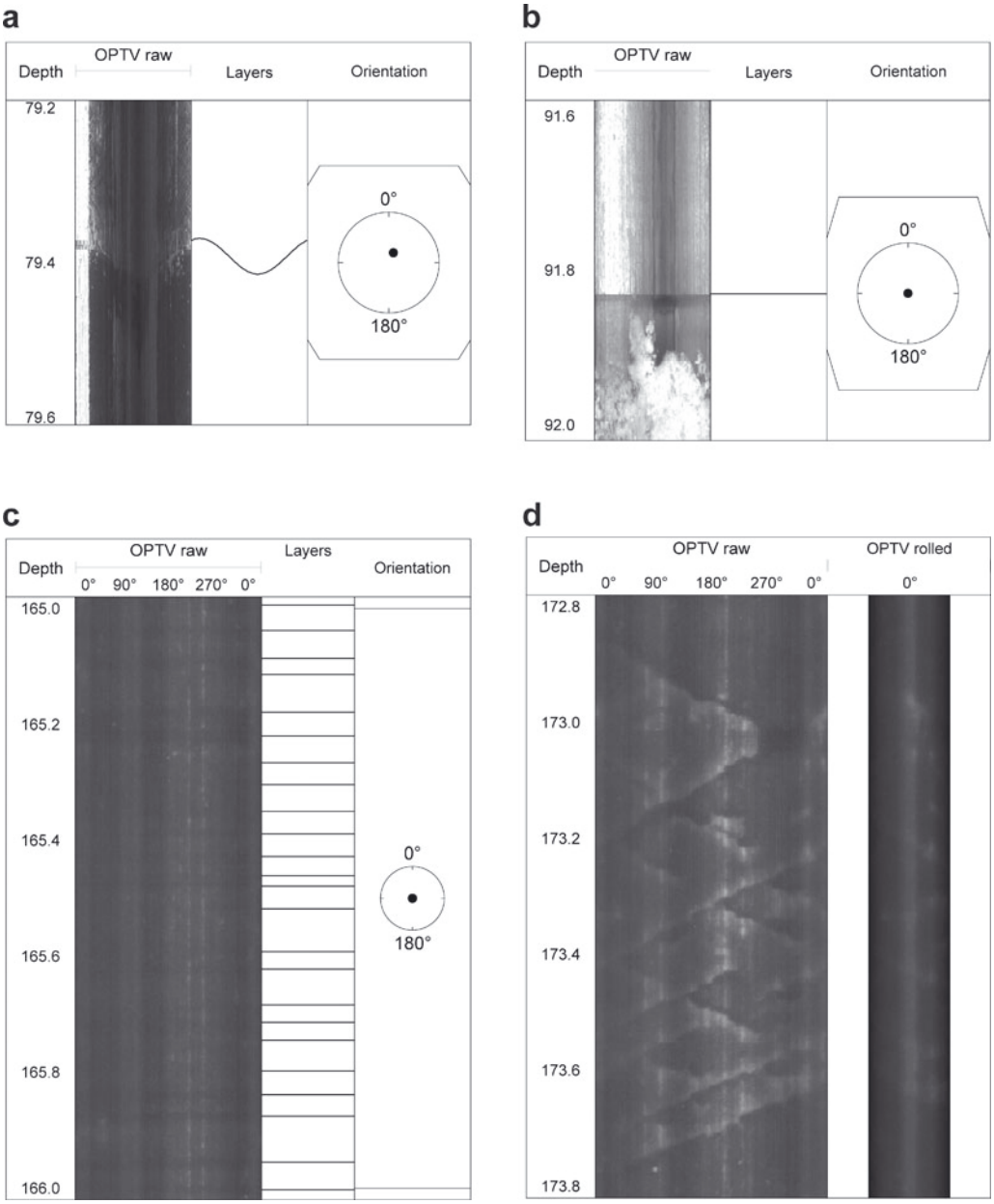

Fig. 3. Details of the NEEM deep borehole OPTV log shown in Figure 1: (a) casing joint at ~79.4 m depth with the sinusoid representing the join on the raw image presented under 'Layers' and the pole to its plane plotted on a lower-hemispheric equal-area projection under 'Orientation'; (b) fluid level, forming a perfectly horizontal plane at a log depth of ~91.8 m. Note the cloudy appearance of scatterers interpreted as suspended ice chips just below the fluid level; (c) regularly repeated horizontal light and dark layers, interpreted as annual layers, at a log depth of ~165 m; and (d) sawtooth patterning, interpreted as drill-cutter scoring, on the borehole wall at a log depth of ~173 m.

cores recovered from the Roi Baudouin ice shelf, Antarctica (Hubbard and others, 2012; Pattyn and others, 2012).

As well as this general decrease in luminosity, however, the OPTV log of the shallow borehole at NEEM also clearly shows regularly repeated layering along its full length. Each such layer has been picked automatically and checked or amended manually using Borehole and Ice Feature Annotation Tool (BIFAT) software (Malone and others, 2013). The number of such layers per metre along the borehole is presented in Figure 4 and a detailed view of a 2 m long section of this log is presented in Figure 5. As with the regular layering revealed in the OPTV log of the deep borehole (Section 3.1), and consistent with the interpretation of borehole video images recorded elsewhere (Hawley and others, 2003; Hawley and Morris, 2006), we interpret this layering as primary stratification or annual layering. At NEEM, being located in the dry-snow zone, such layering forms from a general seasonal contrast between dense wind-packed snow deposited in the winter and a less dense layer influenced by depth hoar formed in the summer. The ~0.5 m spacing of these layers at the top of the shallow borehole log (Fig. 4) is in close agreement with independent estimates of mass accumulation in the area (Kuramoto and others, 2011; Steen-Larsen and others, 2011), supporting this interpretation. Layer counting of the OPTV log reveals an age–depth record that extends back 312 years to 1696 at the base of the borehole. This OPTV-based age–depth scale can be compared directly with one based on an analysis of the physical properties ($\delta^{18}O$ measurements at 2.5 cm resolution combined with electrical conductivity measurement (ECM)-derived volcanic reference horizons) of an adjacent shallow core recovered in 2007 (Steen-Larsen and others, 2011).

https://doi.org/10.3189/2013AoG64A201 Published online by Cambridge University Press

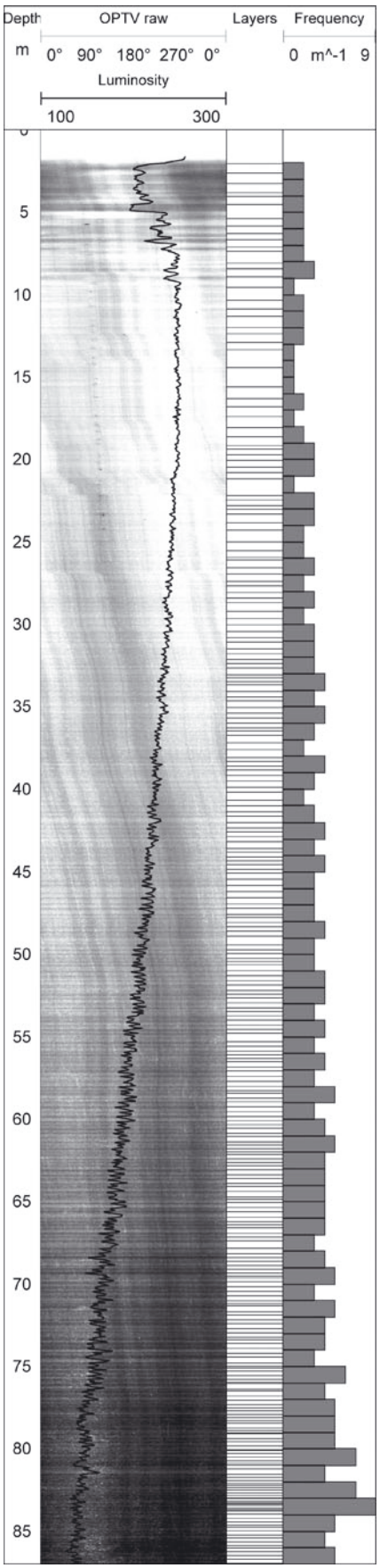

Fig. 4. Complete raw OPTV log of the full length of the NEEM shallow borehole. The raw OPTV image is plotted to the left and is overlain by its non-dimensional luminosity trace sampled each millimetre along the log. The 'first-pass' identification of each individual dark layer (see Fig. 4) is plotted under 'Layers' and their frequency is plotted as a bar chart under 'Frequency'.

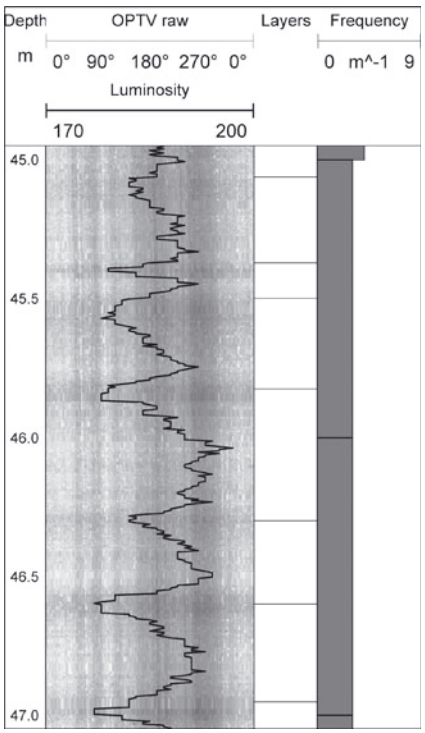

Fig. 5. Detail of the NEEM shallow borehole OPTV log shown in Figure 3.

Scaling the OPTV record to begin in 2007, this comparison reveals that the OPTV-based scale slightly overestimates age relative to the core-based scale (Fig. 6). Thus, summing both records to their deepest common depth at 80 m, the OPTV-derived age extends to 1724, 13 years older than the

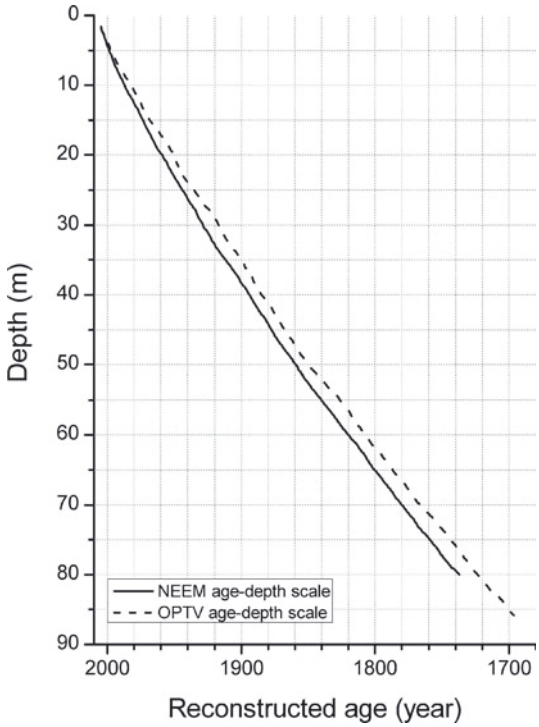

Fig. 6. Age–depth scales derived from the OPTV log (dashed line) and from the analysis of ice-core physical properties (solid line). The OPTV-derived scale plots slightly older than the core-derived scale (investigated further in Fig. 7).

https://doi.org/10.3189/2013AoG64A201 Published online by Cambridge University Press

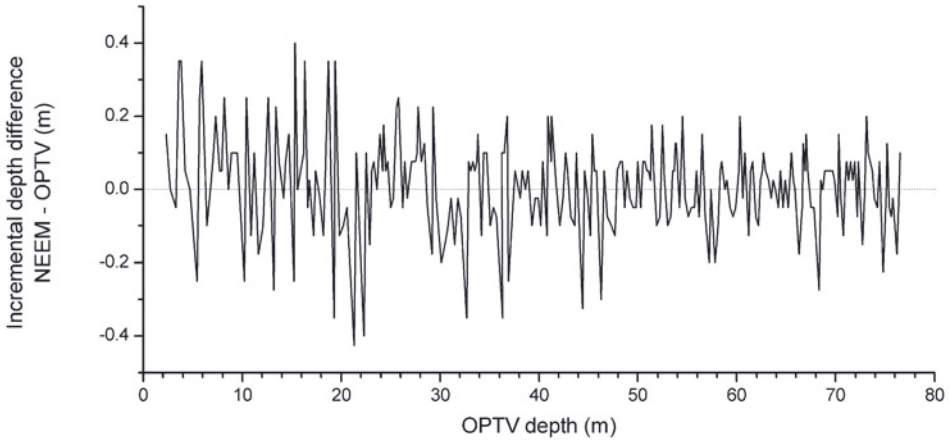

Fig. 7. Bivariate plot of incremental depth differences between the OPTV age–depth scale and the core-derived age–depth scale for each individual year (OPTV – core) plotted against OPTV log depth. Note that the deviation between the two records is largest within the top 30 m of the OPTV log and that there is negligible net deviation below this level.

core-based date of 1737. However, further analysis reveals that this deviation does not accumulate uniformly along the full length of the OPTV log. Plotting the incremental difference in depth between the two scales for each year of the record against depth along the OPTV log (Fig. 7) reveals that there is no net difference in accumulated age between the two records at depths below ~30 m, i.e. all of the age overestimation in the OPTV record occurs in the uppermost 30 m of the log. This zone corresponds closely with that characterized by very high luminosity in the OPTV record (Fig. 4), as discussed above, thereby reducing the accuracy of annual-layer identification. It may also be possible that light–dark couplets, caused by individual depth-hoar events that do not correspond to full seasonal cycles, are erroneously identified as annual layers in the OPTV record in this uppermost zone where high depositional resolution is achieved by widely spaced annual layers.

4. SUMMARY AND CONCLUSIONS

OPTV has been successfully applied to log the uppermost 630 m of the NEEM deep borehole and a nearby shallow borehole. The former involved deploying the instrument in Estisol–Coasol borehole fluid at temperatures as low as ~–28°C. The resulting logs have successfully imaged several borehole properties, both natural and artificial/drilling-related. In the deep borehole, these include:

1. the integrity and dip of casing sections and section joins
2. the borehole fluid level
3. aggregates of ice chips suspended within the borehole fluid
4. sawtooth scores from drill teeth preserved on the borehole wall
5. intermittent sections of layering – assumed to be annual – in ice, at least to a depth of approaching 200 m.

Properties successfully imaged in the shallow borehole include the following:

1. An initial increase (over the uppermost ~10 m) followed by a general decrease in material reflectance with depth.
2. Annual layering in snow and firn along the full length of the borehole (i.e. at least to 87 m depth), accounting for a time period of 312 years (i.e. back to 1696).
3. An age–depth scale that corresponds closely with an independent age–depth scale reconstructed from core-based $\delta^{18}O$ and ECM measurements. A slight over-estimation in the OPTV-derived age relative to the core-based age accrues in the uppermost 30 m of the OPTV log where layer-counting is hampered by very high luminosity in the OPTV image.

It is clear from these results that OPTV-based borehole logging can make a useful contribution to deep ice-coring programmes, including deriving age–depth scales at least to the firn–ice transition and quite probably deeper. As well as imaging natural material properties, OPTV can be used as an effective inspection tool to assist drill crews. Continuing development of our OPTV-based methods will extend this capability with (1) enhanced depth capacity (now operational), (2) high-resolution comparison of OPTV-derived luminosity with snow and firn density (underway) and (3) system adaptation to introduce the option of a variable camera aperture or borehole illumination to improve layer imaging over a range of background luminosities for the construction of age–depth scales (planned).

ACKNOWLEDGEMENTS

This work was supported by the UK Royal Society (RG1430), the Climate Change Consortium of Wales (C3W), the UK Natural Environment Research Council (NE/J013544) and the NEEM Science Consortium. The extended dating of the 2007 shallow core was kindly provided by Henrik B. Clausen and Bo M. Vinther of the Centre for Ice and Climate, Niels Bohr Institute, University of Copenhagen, Denmark. NEEM is directed and organized by the Center of Ice and Climate at the Niels Bohr Institute and the US National Science Foundation (NSF), Office of Polar Programs (OPP). It is supported by funding agencies and institutions in Belgium (FNRS-CFB and FWO), Canada (NRCan/GSC), China (CAS), Denmark (FIST), France (IPEV, CNRS/INSU, CEA and ANR), Germany (AWI), Iceland (RannIs), Japan (NIPR), Korea (KOPRI), The Netherlands

https://doi.org/10.3189/2013AoG64A201 Published online by Cambridge University Press

(NWO/ALW), Sweden (VR), Switzerland (SNF), the UK (NERC) and the USA (US NSF, OPP).

REFERENCES

Bohren CF and Barkstrom BR (1974) Theory of the optical properties of snow. *J. Geophys. Res.*, **79**(30), 4527–4535

Hawley RL and Morris EM (2006) Borehole optical stratigraphy and neutron-scattering density measurements at Summit, Greenland. *J. Glaciol.*, **52**(179), 491–496 (doi: 10.3189/172756506781828368)

Hawley RL, Waddington ED, Alley RA and Taylor KC (2003) Annual layers in polar firn detected by borehole optical stratigraphy. *Geophys. Res. Lett.*, **30**(15), 1788 (doi: 10.1029/2003GL017675)

Hubbard B, Roberson S, Samyn D and Merton-Lyn D (2008) Digital optical televiewing of ice boreholes. *J. Glaciol.*, **54**(188), 823–830 (doi: 10.3189/002214308787779988)

Hubbard B, Tison J-L, Pattyn F, Dierckx M, Boereboom T and Samyn D (2012) Optical-televiewer-based identification and characterization of material facies associated with an Antarctic ice-shelf rift. *Ann. Glaciol.*, **53**(60), 137–146 (doi: 10.3189/2012AoG60A045)

Johnsen SJ and 16 others (2007) The Hans Tausen drill: design, performance, further developments and some lessons learned. *Ann. Glaciol.*, **47**, 89–98 (doi: 10.3189/172756407786857686)

Kinnard C and 7 others (2008) Stratigraphic analysis of an ice core from the Prince of Wales Icefield, Ellesmere Island, Arctic Canada, using digital image analysis: high-resolution density, past summer warmth reconstruction, and melt effect on ice core solid conductivity. *J. Geophys. Res.*, **113**(D24), D24120 (doi: 10.1029/2008JD011083)

Kuramoto T and 6 others (2011) Seasonal variations of snow chemistry at NEEM, Greenland. *Ann. Glaciol.*, **52**(58), 193–200 (doi: 10.3189/172756411797252365)

Malone T, Hubbard B, Merton-Lyn D, Worthington P and Zwiggelaar R (2013) Borehole and Ice Feature Annotation Tool (BIFAT): a program for the automatic and manual annotation of glacier borehole images. *Comput. Geosci.*, **51**, 381–389 (doi: 10.1016/j.cageo.2012.09.002)

Obbard RW, Cassano T, Aho K, Troderman G and Baker I (2011) Using borehole logging and electron backscatter diffraction to orient an ice core from the Upper Fremont Glacier, Wyoming, USA. *J. Glaciol.*, **57**(205), 832–840 (doi: 10.3189/002214311798043762)

Pattyn F and 8 others (2012) Melting and refreezing beneath Roi Baudouin Ice Shelf (East Antarctica) inferred from radar, GPS and ice-core data. *J. Geophys. Res.*,**117**(F4), F04008 (doi: 10.1029/2011JF002154)

Roberson S and Hubbard B (2010) Application of borehole optical televiewing to investigating the 3-D structure of glaciers: implications for the formation of longitudinal debris ridges, Midre Lovénbreen, Svalbard. *J. Glaciol.*, **56**(195), 143–156 (doi: 10.3189/002214310791190802)

Siddans AWB (2002) Structural geology using borehole wall imagery: case study of an OPTV log in flagstones, North Scotland. *First Break*, **20**(10), 623–629

Steen-Larsen HC and 23 others (2011) Understanding the climatic signal in the water stable isotope records from the NEEM shallow firn/ice cores in northwest Greenland. *J. Geophys. Res.*, **116**(D6), D06108 (doi: 10.1029/2010JD014311)